Generation of Microcellular Polyurethane with Supercritical Carbon Dioxide

Shunsuke Ito, Katsuji Matsunaga, Masahiro Tajima, Yasuhiko Yoshida

Department of Applied Chemistry, Faculty of Engineering, Toyo University, 2100 Kujirai, Kawagoe-Shi, Saitama 350-8585, Japan

Received 15 August 2006; accepted 6 June 2007
DOI 10.1002/app.26854
Published online 28 August 2007 in Wiley InterScience (www.interscience.wiley.com).

ABSTRACT: We examined the formation of microcellular foam in a thermoplastic polyurethane elastomer (TPU) with supercritical carbon dioxide. Measurements of the permeability and impregnation with carbon dioxide suggested that the impregnation of TPU with carbon dioxide was affected by the soft-segment chain length and soft-segment concentration in TPU and that carbon dioxide was mainly present in the soft-segment area. Thus, it seemed likely that the nucleation and growth of the nuclei in the microcells occurred in the soft-segment area. In addition, scanning electron microscopy of the microcells indicated that the higher the saturation pressure was, the smaller the mean cell diameter was; that is, the higher the cell number density was, the lower the foaming temperature was, the smaller the mean cell diameter was, and the lower the saturation pressure was, the more conspicuous this phenomenon was. These results showed that the saturation pressure and foaming temperature affected the cell structure. © 2007 Wiley Periodicals, Inc. J Appl Polym Sci 106: 3581–3586, 2007

Key words: microstructure; nucleation; polyurethanes

INTRODUCTION

Microcellular foam (MCF) comprises closed cells with a cell diameter of 10 μm or less and a cell number density of 10^9–10^{15} cells/cm^3. To date, many studies of MCF have been reported based on the theory that the material can be reduced without the lowering of its physical strength by the insertion of numerous voids, which are smaller than defects, into the polymer.[1–20] Although conventional plastic foam is light because of its large cell diameter and low cell number density, it has low physical strength and limited uses. MCF is expected to be used for various purposes because of its lightness, heat-insulating properties, shock-absorbing properties, and electrical and resource-saving characteristics.

MCF is produced[1] by a sharp reduction of the pressure to atmospheric pressure and an increase in the temperature after the saturation of a polymer with an inert gas (carbon dioxide or nitrogen). Thus, the thermodynamic stability of the polymer is lost, and at the same time, cell nuclei are formed in the polymer. The difference in pressure between the inside and outside of the material is the driving force for the growth of cell nuclei, and the growth stops when the internal and external pressures equilibrate.

Correspondence to: S. Ito (shun_ito55@yahoo.co.jp).

Journal of Applied Polymer Science, Vol. 106, 3581–3586 (2007)

The materials used to produce MCF include polystyrene, polypropylene, poly(ethylene terephthalate), polycarbonate, poly(methyl methacrylate), poly(vinyl chloride), styrene–acrylonitrile copolymer, and acrylonitrile–butadiene–styrene copolymer.[2–18] Furthermore, studies have been conducted on the mechanical strength of MCF,[11,19] the biodegradability of MCF,[20] and so forth.

In general, a supercritical fluid exists as a noncondensable, high-density fluid above the critical temperature and critical pressure. Supercritical fluids have the properties of high diffusivity, high density, low viscosity, and so forth and are characterized by continuous changes in these properties. On the basis of these properties and characteristics, supercritical fluids are used for extraction, isolation, degradation, and reaction and as ingredients. Because carbon dioxide is nontoxic, nonflammable, and inexpensive and readily becomes supercritical (31.1°C and 7.38 MPa), it is widely used for extraction and isolation, as an alternative to organic solvents, and as an ingredient. The use of supercritical carbon dioxide as a foaming agent reduces the duration and increases the amount of impregnation of a material with gas. Furthermore, as the relationship between polymer expansion through the dissolution of carbon dioxide and the drop in the glass-transition temperature shows,[21,22] low-temperature foam molding through a plasticization effect[23] of carbon dioxide on a polymer can be observed.

A thermoplastic polyurethane elastomer (TPU) is a block copolymer that is composed of alternating soft

and hard segments. The soft segment is a polyol with an ether or ester group in the main chain, which mediates the flexibility of the elastomer. The hard segment contains urethane linkages generated by the reaction of diisocyanate and short-chain diols and influences the mechanical properties, such as the elasticity, hardness, and tearing strength. Because hydrogen bonding occurs between the hard segments, the soft segment and the hard segment are incompatible with each other and form a phase-separation structure. Through changes in the quantity and structure of these two components, different types of TPUs can be obtained and used for different purposes, such as automobile parts, building materials, sports goods, and medical equipment.

To date, there have been few reports on polyurethane MCF.[24,25] Once the production of MCF using polyurethane is established, the uses should increase dramatically. Accordingly, in this study, we initially used measurements of the gas permeability and the quantity of impregnated carbon dioxide to determine the existence area (soft or hard segment) of carbon dioxide needed for the nucleation and growth of nuclei in TPUs, with the aim of producing MCF in TPUs with supercritical carbon dioxide. Then, using supercritical carbon dioxide as a foaming agent, we examined the effects of the temperature and saturation pressure on the process of introducing microcells into TPUs and on the cell structure.

EXPERIMENTAL

Materials

The following chemicals were used: the polyol poly (oxytetramethylene) α,ω-diol [PTMG; number-average molecular weight (M_n) = 1000, 2000, or 3000; Hodogaya Chemical Co., Ltd., Japan], the diisocyanate hexamethylene diisocyanate (Tokyo Chemical Industry Co., Ltd., Japan), and the chain extender 1,3-propanediol (PD; Kanto Chemical Co., Inc., Japan). TPUs with different soft-segment concentrations were synthesized through the variation of M_n of the polyol and the molar ratio of the polyol, diisocyanate, and chain extender.

Synthesis

TPU synthesis was conducted according to the prepolymer technique. An isocyanate-terminated urethane prepolymer was obtained by the addition of a certain amount of diisocyanate to the vacuum-dried polyol and mixing at 100°C for 90 min. A certain amount of PD was added to the prepolymer; the mixture was mixed vigorously for 2 min and cured at 100°C for 24 h.

Thermal analyses

The thermal behaviors of the TPUs were measured with aluminum cells at a rate of temperature increase of 5°C/min with a measurement range of −130 to 250°C in a nitrogen atmosphere with a model DSC220 differential scanning calorimeter (Seiko Instruments, Inc., Japan).

Gas permeability measurements

The gas permeability coefficient [P (barrer)] of a TPU, with the thickness adjusted to 1 mm with a model HP-100TE hot press (Nisshin Kagaku Kogyo Co., Ltd., Japan), was determined by the assessment of its permeability at the measurement temperature of 31.1°C with a model MT-C1 gas permeability apparatus (Toyoseiki Co., Ltd., Japan) after 24-h vacuuming. The diffusion coefficient [D (cm^2/s)] and solubility coefficient [S ($cm^3\ cm^{-3}\ cmHg^{-1}$)] were then determined from eqs. (1) and (2):

$$P = D \times S \tag{1}$$

$$D = d^2/6t \tag{2}$$

where d represents the TPU thickness (cm) and t represents the time taken for diffusion (s).

CO_2 impregnation measurements

A specimen of 10 mm × 10 mm was cut from the 1-mm-thick TPU. The specimen was placed with a certain amount of dry ice in a model MMJ-200 autoclave (OM Lab-Tech Co., Ltd., Japan) and impregnated with carbon dioxide at 40°C for 1–25 h under a pressure of 2–10.5 MPa. The quantity of impregnation with carbon dioxide was determined from the difference in the weights before and after impregnation.

Foaming

A specimen with dimensions of 10 mm × 10 mm × 1 mm (length × width × thickness) was placed in an autoclave with a certain amount of dry ice and was impregnated with carbon dioxide at 40°C under a pressure of 5–10 MPa for about 6 h. After a drastic pressure reduction to atmospheric pressure, the specimen was removed from the autoclave, soaked at 100–120°C in glycerin for 20 s, and cooled in an ice–water bath.

Determination of the cell number density

The specimen was frozen in liquid nitrogen and cracked. The fracture surface was coated with gold with ion-sputtering equipment (model SC-701, Sanyu

TABLE I
Thermal Behavior and CO_2 Gas Permeability, Diffusivity, and Solubility of the TPUs

M_n of PTMG	Molar ratio[a]	SSC (%)[b]	T_{gs} (°C)[c]	T_{ms} (°C)[d]	T_{mh} (°C)[e]	P (bar)	D (10^{-7} cm^2s)	S ($10^{-4}/cm^3/cm^{-3}/cmHg^{-1}$)
1000	1.0/4.3/3.3	50	−68.4	10.2	150.7	17.6	9.31	18.9
	1.0/2.9/1.9	60	−67.1	12.1	142.1	27.1	12.2	22.3
	1.0/1.9/0.9	70	−68.2	11.1	123.8	37.6	15.4	24.4
	1.0/1.2/0.2	80	−70.4	17.3	112.8	48.8	19.0	25.6
	1.0/4.0/3.0	51.8	−69.7	11.1	150.7	22.7	10.3	22.0
2000	1.0/8.0/7.0	50	−72.7	8.4	159.7	28.5	12.8	22.3
	1.0/5.4/4.4	60	−72.4	7.5	154.3	37.3	18.2	20.5
	1.0/3.5/2.5	70	−73.5	19.2	150.7	49.1	25.9	19.0
	1.0/2.1/1.1	80	−71.5	22.7	125.6	59.6	38.9	15.3
	1.0/4.0/3.0	67.1	−70.7	19.2	157.0	46.8	23.3	20.1
3000	1.0/12/11	50	−78.2	21.8	157.9	—	—	—
	1.0/8.2/7.2	60	−76.4	23.6	158.7	43.2	18.3	23.6
	1.0/5.3/4.3	70	−73.3	22.7	158.8	53.8	21.6	24.9
	1.0/3.2/2.2	80	−75.5	24.5	142.6	71.1	31.1	22.8
	1.0/4.0/3.0	75.8	−75.0	23.6	144.4	61.3	26.9	22.8

[a] Polyol/diisocyanate/chain extender.
[b] Soft-segment concentration.
[c] Glass-transition temperature of the soft segment.
[d] Melting point of the soft segment.
[e] Melting point of the hard segment.

Electron Co., Ltd., Japan). The fracture surface was examined with a model JSM-5310LV scanning electron microscope (JEOL, Ltd., Japan). From the scanning electron microscopy images, the cell count and mean cell diameter were determined, and the cell number density was determined with the following equations:[2]

$$N_f = (n/A)^{3/2} \tag{3}$$

$$V_f = \pi/6 \times D_A^3 N_f \tag{4}$$

$$N_0 = N_f/(1 - V_f) \tag{5}$$

where N_f represents the cell number density in the foamed polymer (cm^{-3}), n represents the cell count in the analysis range, A represents the analysis range (cm^2), V_f represents the volume fraction of cells in the foamed polymer (cm^3 of cell/cm^3 of foam), D_A represents the mean cell diameter (cm), and N_0 represents the cell number density in the polymer before foam formation (cells/cm^3). The cell number density of the specimen after foam formation was evaluated with eq. (5) to eliminate the effects of differences in the multiplying factor for foam formation.

RESULTS AND DISCUSSION

The permeability behavior of carbon dioxide was examined with TPUs for which M_n of the polyol and the component ratios of the soft segment to hard segment were changed (Table I). The higher M_n was for the polyol, the higher P and D were for the TPUs. This probably reflects increases in the chain free volume and diffusivity due to an increase in the number of the oxytetramethylene units that made up the soft-segment chain. It has been reported that the gas permeability of a TPU affects the chain length of the soft segment.[26–29] McBride et al.[26] showed by measurements of the gas permeability for ether or ester TPUs that the gas diffusivity affects the amount of the hard segment, the chain length of the soft segment, and the type of soft segment. Furthermore, Xiao et al.[27] showed that the amount of the hard segment and the chain length of the soft segment affect the gas permeability of TPUs. Galland et al.[28] measured the gas permeability of TPUs with different M_n values, PTMG as a polyol, and five types of gases, and they showed that the gas diffusivity depends on the soft-segment chain. Matsunaga et al.[20] showed that the molecular structure or M_n of the polyol affects the gas diffusibility. As shown in Table I, an improvement in the diffusivity can be observed after an increase in the soft-segment concentration. Differential scanning calorimetry measurements show that the temperature of the soft segment is above the melting temperature during the gas permeability measurements. This means that the soft-segment chain is mobile and that the gas can pass through the spaces between the molecular chains. On the basis of the findings that the melting point of the hard segment is much higher than the measurement temperature and that the hard segment is of the domain structure formed by hydrogen bonding between urethane groups and intermolecular interactions, it appears that gas diffusion in the hard segment is very limited. Because no conspicuous differences in

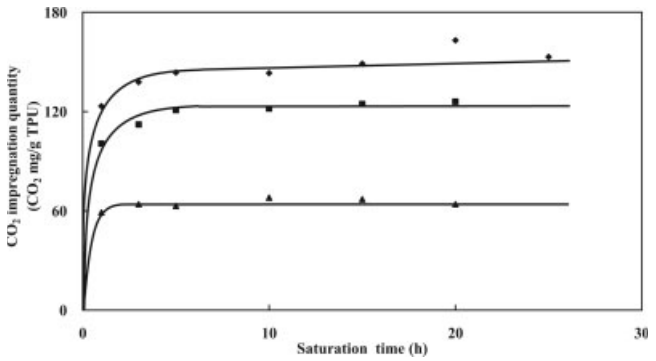

Figure 1 CO_2 impregnation for the three TPU soft-segment lengths as a function of the saturation time (polyol/diisocyanate/chain extender molar ratio = 1 : 4 : 3; saturation pressure = 8 MPa; saturation temperature = 40°C): (▲) PTMG1000-based TPU, (■) PTMG2000-based TPU, and (◆) PTMG3000-based TPU.

S have been observed among the various types of TPUs, we conclude that the diffusivity has an effect on the gas permeability behavior in the TPUs. Accordingly, it seems that the increase in the concentration of the soft segment has an effect on the diffusivity, which leads to an improvement in the gas permeability. Thus, it is suggested that in the course of gas permeation of TPUs, carbon dioxide selectively diffuses and permeates the soft segment.

Figure 1 shows the rates of carbon dioxide impregnation of TPUs with polyols of different molecular weights. The amount of impregnation increases as the molecular weight of the polyol increases. The increase in the free volume of the soft-segment chain and the decrease in the quantity of the hard segment due to the lengthening of the soft-segment chain affect the amount of carbon dioxide impregnation of the TPUs. As for the amount of the hard segment, it has been reported that a decrease in the quantity of the hard segment increases the amount of carbon dioxide impregnation of a TPU.[30] The soft segment seems to be the main area impregnated with carbon dioxide on the basis of the relationship between the chain length of the soft segment and the amount of impregnation. From these results, it is clear that the gas permeation behavior correlates with the amount of impregnation of a TPU with carbon dioxide, and it is suggested that carbon dioxide is mainly present in the soft-segment area. Thus, it is likely that the nucleation and growth of nuclei in MCF take place mainly in the soft-segment area.

Figure 2 shows the relationship between the saturation pressure and the amount of carbon dioxide impregnation of a PTMG3000-based TPU. When the pressure is equal to or less than 6 MPa, the saturation pressure is proportional to the amount of impregnation, and when the pressure is equal to or more than 7 MPa, the amount of impregnation increases dramatically. At a pressure equal to or more than 7 MPa, carbon dioxide is in the supercritical state, and it appears that the absorption of carbon dioxide facilitates plasticization or swelling and increases the amount of impregnation.

Figure 3 shows the internal structure of a foamed TPU. The electron micrograph reveals that the TPU comprises numerous microcells. Although the inside of the TPU contains microcells, there are none on the surface. It appears that a sudden temperature change in the foaming of a TPU affects the gas diffusion rate and the growth rate of nuclei both inside and on the surface of a TPU. Figure 4 shows the relationship between the mean cell diameter and saturation pressure, and Figure 5 shows the relationship between the cell number density and saturation pressure. The higher the saturation pressure is, the smaller the mean cell diameter is and the higher the cell number density is. We hypothesize that with an increase in the saturation pressure, the activation energy for nucleation decreases, and this leads to an increase in the cell number density. In addition, the increase in the saturation pressure probably causes the rate of nucleation to increase exponentially, and this leads to a decrease in the availability of the gas needed for growth of the bubble nuclei and reduces the mean cell diameter. At a pressure of 5 MPa, the higher the foaming temperature is, the greater the mean cell diameter is, but at higher saturation pressures, this effect is smaller. The lower the saturation pressure is, the lower the number is of nuclei formed. Therefore, it appears that a rise in the foaming temperature causes a drop in the polymer viscosity and increases the effect on the cell diameter.

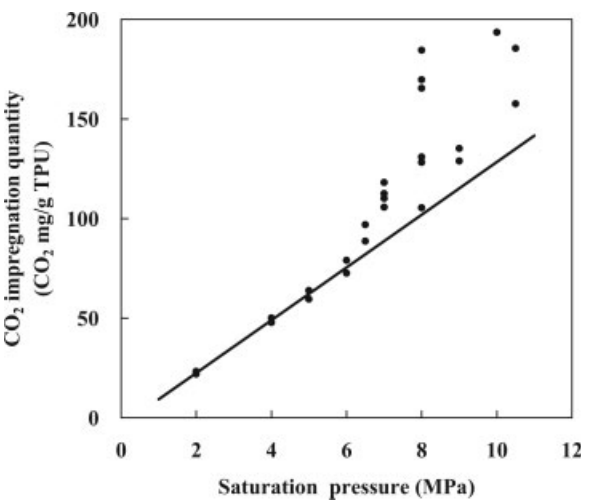

Figure 2 CO_2 impregnation as a function of the saturation pressure for PTMG3000-based TPU (polyol/diisocyanate/chain extender molar ratio = 1 : 4 : 3; saturation temperature = 40°C; saturation time = 12 h).

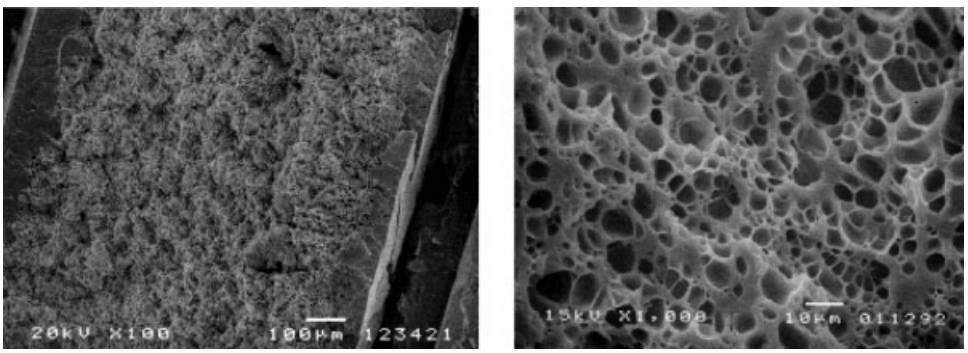

Figure 3 Scanning electron micrographs of PTMG3000-based TPU (polyol/diisocyanate/chain extender molar ratio = 1 : 4 : 3; blowing temperature = 120°C; saturation pressure = 8 MPa; saturation temperature = 40°C; saturation time = 6 h).

Furthermore, it appears that an increase in the saturation pressure causes an exponential increase in the number of nuclei formed and reduces the gas supply, and this reduces the effect on the cell diameter.

CONCLUSIONS

We have examined the production of MCF, using supercritical carbon dioxide, and investigated the effects on the cell structure. The measurements of the carbon dioxide permeability show that the gas diffusivity increases because of increases in the chain length and concentration of the soft segment. Furthermore, the measurements of the amount of carbon dioxide impregnation show that the amount of carbon dioxide impregnation increases with an increase in the chain length of the soft segment. These results show that the carbon dioxide permeability correlates with the amount of impregnation and suggest that carbon dioxide is mainly present in the soft-segment area. Thus, it appears that the nucleation and growth of nuclei in MCF composed of a TPU take place mainly in the soft-segment area. Meanwhile, the amount of supercritical carbon dioxide impregnation improves dramatically. After the impregnation of a TPU with carbon dioxide under high pressure, MCF with a high cell number density develops. It has been shown that changes in the saturation pressure result in cell structure changes, and the higher the pressure is, the smaller the cell diameter is and the higher the cell number density is of MCF.

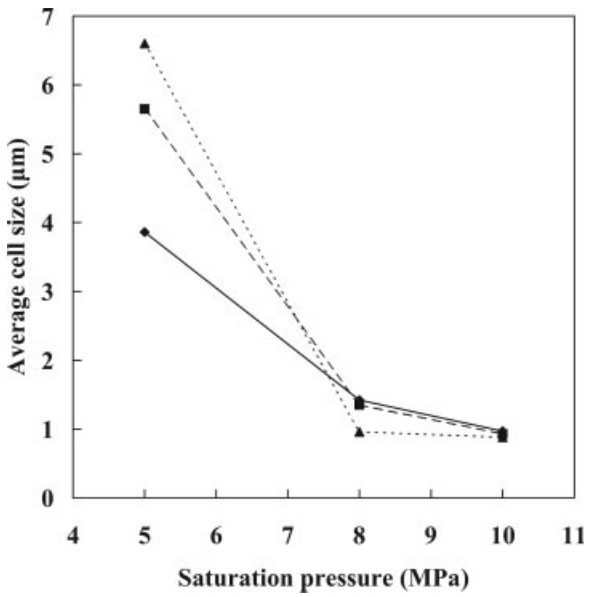

Figure 4 Plot of the average cell size as a function of the saturation pressure for PTMG3000-based TPU (polyol/diisocyanate/chain extender molar ratio = 1 : 4 : 3). The blowing temperatures were (◆) 100, (■) 110, and (▲) 120°C.

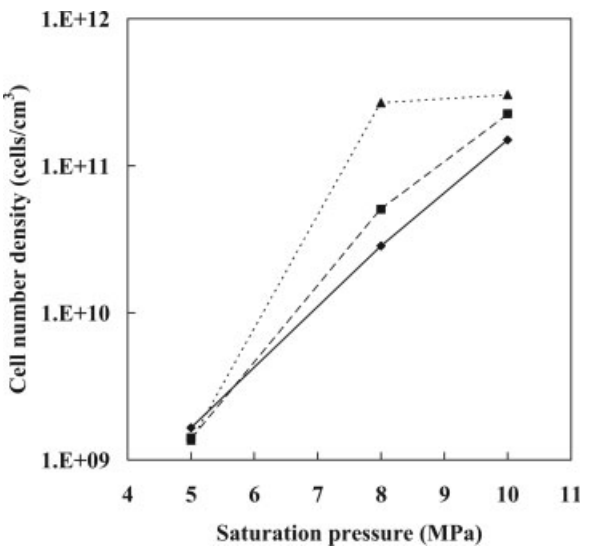

Figure 5 Plot of the cell number density as a function of the saturation pressure for PTMG3000-based TPU (polyol/diisocyanate/chain extender molar ratio = 1 : 4 : 3). The blowing temperatures were (◆) 100, (■) 110, and (▲) 120°C.

APPENDIX

Nucleation within a polymer is classified as uniform nucleation or nonuniform nucleation.[1,2,11] Uniform nucleation refers to the case in which gas molecules that are dissolving in the polymer form a second phase of stable cells. Nonuniform nucleation refers to the case in which cells are formed at the interface between the polymer and additive. Colton and Suh[1,2] expressed the state of uniform nucleation in the following equations. The cell number density resulting from uniform nucleation (N_{HOM}) is shown in eq. (A.1), and the activation energy for nucleation (ΔG^*) is shown in eq. (A.2):

$$N_{HOM} = C_0 \cdot f_0 \exp \frac{-\Delta G^*}{KT} \tag{A.1}$$

$$\Delta G^* = \frac{16\pi\gamma^3}{3(P_S - P_0)^2} \tag{A.2}$$

where C_0 represents the gas molecule density (cm^3/g), f_0 represents the frequency constant of the clustering of gas molecules around the nuclei, K represents the Boltzmann constant, T represents the temperature, γ represents the surface formation energy, P_S represents the saturation pressure (Pa), and P_0 represents the environmental pressure (Pa). Equations (A.1) and (A.2) show that the higher the saturation pressure is, the lower ΔG^* is and the higher N_{HOM} is.

References

1. Colton, J. S.; Suh, N. P. Polym Eng Sci 1987, 27, 485.
2. Colton, J. S.; Suh, N. P. Polym Eng Sci 1987, 27, 493.
3. Kumar, V.; Suh, N. P. Soc Plast Eng Tech Pap 1998, 44, 715.
4. Kweeder, J. A.; Ramesh, N. S.; Campbell, G. A.; Rasmussen, D. H. Soc Plast Eng Tech Pap 1991, 37, 1398.
5. Ramesh, N. S.; Rasmussen, D. H.; Campbell, G. A. Polym Eng Sci 1991, 31, 1657.
6. Colton, J. S. Plast Eng 1988, 44, 53.
7. Kumar, V.; Suh, N. P. Polym Eng Sci 1990, 30, 1323.
8. Arora, K. A.; Lesser, A. J.; McCarthy, T. J. Polym Eng Sci 1998, 38, 2055.
9. Baldwin, D. F.; Park, C. B.; Suh, N. P. Polym Eng Sci 1996, 36, 1437.
10. Sato, Y.; Chikatsune, T.; Hayashi, K.; Takishima, S.; Masuoka, H.; Yamamoto, H.; Takasugi, M. Seikei Kako 2004, 16, 247.
11. Kumar, V.; Weller, J. E. Cellul Microcellul Mater 1996, 76, 17.
12. Kumar, V.; Weller, J. E. Soc Plast Eng Tech Pap 1991, 37, 1401.
13. Goel, S. K.; Beckman, E. J. Cellul Polym 1993, 12, 251.
14. Goel, S. K.; Beckman, E. J. Polym Eng Sci 1994, 34, 1137.
15. Kumar, V.; Weller, J. E.; Montecillo, R. Soc Plast Eng Tech Pap 1992, 38, 1452.
16. Kumar, V.; Weller, J. E. Polym Mater Sci Eng 1992, 67, 501.
17. Lee, K. N.; Suh, Y. J.; Lee, H. J.; Kim, J. H. Polym Mater Sci Eng 1991, 80, 161.
18. Kumar, V.; Weller, J. E.; Murray, R. Annu Tech Conf 1995, 41, 2202.
19. Shimbo, M.; Baldwin, D. F.; Suh, N. P. Seikei Kako 1994, 6, 863.
20. Sparacio, D.; Beckman, E. J. ACS Symp Ser 1998, 713, 181.
21. Sefcik, M. D. J Polym Sci Part B: Polym Phys 1986, 24, 957.
22. Kamiya, Y.; Hirose, T.; Naito, Y.; Mizoguchi, K. J Polym Sci Part B: Polym Phys 1988, 26, 159.
23. Zhang, Z.; Handa, Y. P. J Polym Sci Part B: Polym Phys 1998, 36, 977.
24. Dai, X.; Liu, Z.; Wang, Y.; Yang, G.; Xu, J.; Han, B. J Supercrit Fluids 2005, 33, 259.
25. Ota, T. Seikei Kako Symp A 1998, 210, 163.
26. McBride, J. S.; Massaro, T. A.; Cooper, S. L. J Appl Polym Sci 1979, 23, 201.
27. Xiao, H.; Ping, Z. H.; Xie, J. W.; Yu, T. Y. J Appl Polym Sci 1990, 40, 1131.
28. Galland, G.; Lam, T. M. J Appl Polym Sci 1993, 50, 1041.
29. Matsunaga, K.; Sato, K.; Tajima, M.; Yoshida, Y. Polym J 2005, 37, 413.
30. Briscoe, B. J.; Kelly, C. T. Polymer 1996, 37, 3405.